

# Synthesis of Triphenylethylene-Naphthalimide Conjugates as topoisomerase-II $\alpha$ inhibitor and HSA binder

Sudesh Rani,<sup>[a]</sup> Vijay Luxami,<sup>[a]</sup> and Kamaldeep Paul<sup>\*[a]</sup>

A series of triphenylethylene-naphthalimide (TPE-naph) conjugates was synthesized by a molecular hybridization technique, and their anticancer activity was evaluated *in vitro* on 60 human cancer cell lines through their cytotoxicity. The ratios of *E* and *Z* isomers were determined on the basis of HPLC methodology and NMR spectroscopy. The structure-activity relationship for anticancer activity was deduced on the basis of the nature and bulkiness of the amine attached to the C-4 position of the naphthalene ring. Experimental and molecular modeling studies of the most active TPE-naph conjugate

bearing a morpholinyl group showed that it was able to inhibit topoisomerase-II (TOPO-II) as a possible intracellular target. Moreover, the transportation behavior of TPE-naph conjugate towards human serum albumin (HSA) indicated efficient binding affinity. The steady-state and time-dependent fluorescent results suggested that this conjugate quenched HSA significantly through static as well as dynamic quenching. Thus, this report discloses the scope of triphenylethylene-naphthalimide (TPE-naph) conjugates as efficient anticancer agents.

## Introduction

Cancer is a cluster of diseases that accounts for leading cause of mortality globally.<sup>[1]</sup> According to cancer reports in 2018, about 17.0 million cancer cases were diagnosed and 9.5 million died worldwide.<sup>[2]</sup> Due to prevalence of cancer, development of potential anti-tumor drugs with optimal physicochemical profile is of utmost importance.<sup>[3]</sup> Long term administration of drug is the main cause of paramount failure in drug discovery and remains prevalent as challenge for contemporary medicinal chemistry.<sup>[4]</sup> Combinational principle or molecular hybridization is the effective way to develop multi-target drug candidates with enhanced biological activities.<sup>[5]</sup> The success of substituted olefins (such as tamoxifen (I), a marketed drug) and naphthalimide (II; such as amonafide, in clinical trials) provoked to synthesize their conjugate molecules in the area of cancer therapy.<sup>[6,7]</sup>

The triphenylethylene (TPE) scaffold viz., tamoxifen, a first-generation selective estrogen receptor modulator (SERM) owing the feature of estrogen diethylstilbestrol has emerged as target motif for the treatment of cancer in pharmacotherapy.<sup>[8,9]</sup> As an anticancer agent, it resists tumor formation either by blocking estrogen receptor or by interacting with factors which impair DNA replication.<sup>[10,11]</sup> On account of partial agonistic character of tamoxifen,<sup>[12]</sup> extensive efforts have been devoted to endow new triarylethylene analogues as potent anticancer agents with increased efficacy and toxicological profile. Adopting the technique of molecular hybridization, coupling of triphenylethylene analogue (tamoxifen) with various pharmacophores

such as coumarin (III) and xanthen (IV) manifested significant anticancer activity (Figure 1).<sup>[13,14]</sup>

On the other hand, naphthalimide is a class of heterocycles, constituting  $\pi$ -deficient planar aromatic structure and a versatile pharmacophore with diverse biological applications in pharmaceuticals such as anticancer, antibacterial, antiviral and analgesic.<sup>[15,16]</sup> Naphthalimides exert antiproliferative activity due to their ability of intercalate into the base pairs of DNA, through DNA-groove binding and topoisomerase (TOPO) inhibition.<sup>[17]</sup> Naphthalimide analogue such as amonafide, has reached in phase II clinical trials and displayed promising anticancer activity.<sup>[18]</sup> But apparently, clinical development of this moiety was impeded due to its neurological toxicity, poor physicochemical property and poor therapeutic index.<sup>[19,20]</sup> Thus, researchers have focused on efforts geared toward the modification of imide position and substituents at C-4 position of naphthalene ring. Rao et al. have synthesized naphthalimide-benzothiazole/cinnamide derivatives (V) as active anticancer agent against lung and colon cancer cell lines as well as inhibiting the topoisomerase-II activity,<sup>[21]</sup> whereas Lu et al. reported a series of C-4 naphthalimide-benzothiazole conjugates (VI) with potent inhibitory activity towards murine melanoma cell lines.<sup>[22]</sup> These promising anticancer activities of naphthalimide and triphenylethylene analogues have prompted us to develop novel structural hybrids evading drug resistance. To the best of our knowledge, no report on triphenylethylene-naphthalimide (TPE-naph) conjugate has been explored as anticancer agents in drug discovery.

In view of these investigations, we designed target hybrid by reducing the flexibility as depicted in Figure 2, by conjugating amino triphenylethylene scaffold to 4-substituted naphthalic anhydride without any linker. Further, triphenylethylene-naphthalimide conjugates substituted with various primary and secondary amines were synthesized and evaluated for their cytotoxicity against 60 human cancer cell lines. As triphenylethylene and naphthalimide derivatives are observed as top-

[a] S. Rani, Dr. V. Luxami, Dr. K. Paul  
School of Chemistry and Biochemistry  
Thapar Institute of Engineering and Technology  
Patiala-147004, Punjab (India)  
E-mail: kpaul@thapar.edu

Supporting information for this article is available on the WWW under <https://doi.org/10.1002/cmdc.202100034>

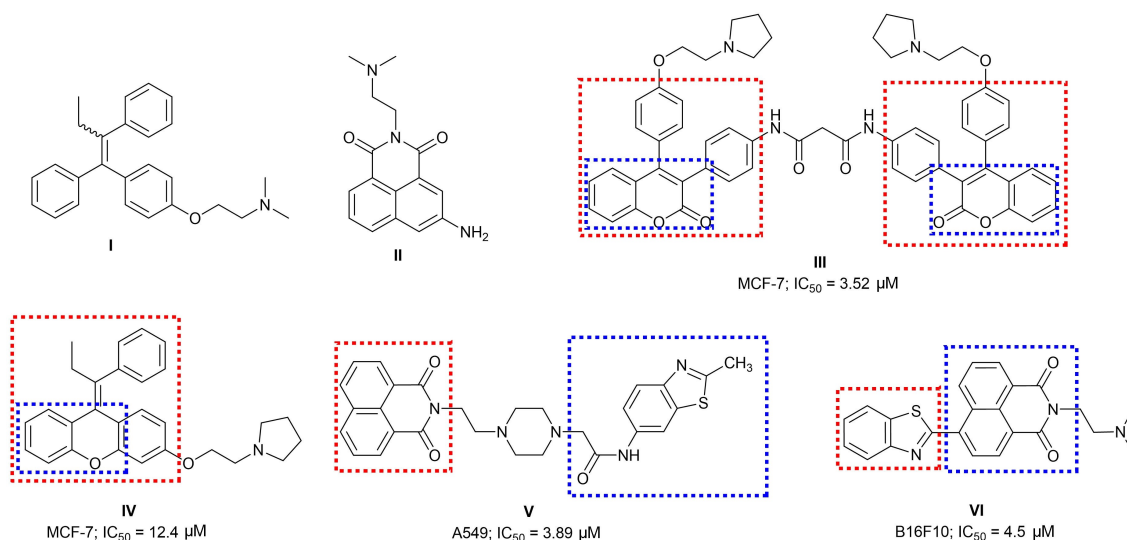


**Figure 1.** Marketed drug tamoxifen (I), drug in clinical trials amonafide (II), lead hybrids based on triphenylethylene (III, IV) and naphthalimide (V, VI).

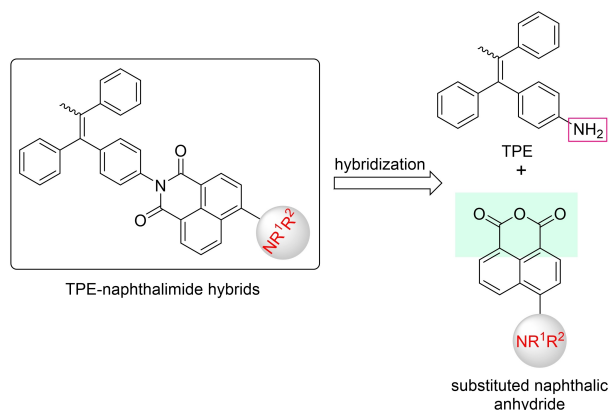


**Figure 2.** Molecular hybridization of TPE with 4-substituted naphthalic anhydride.

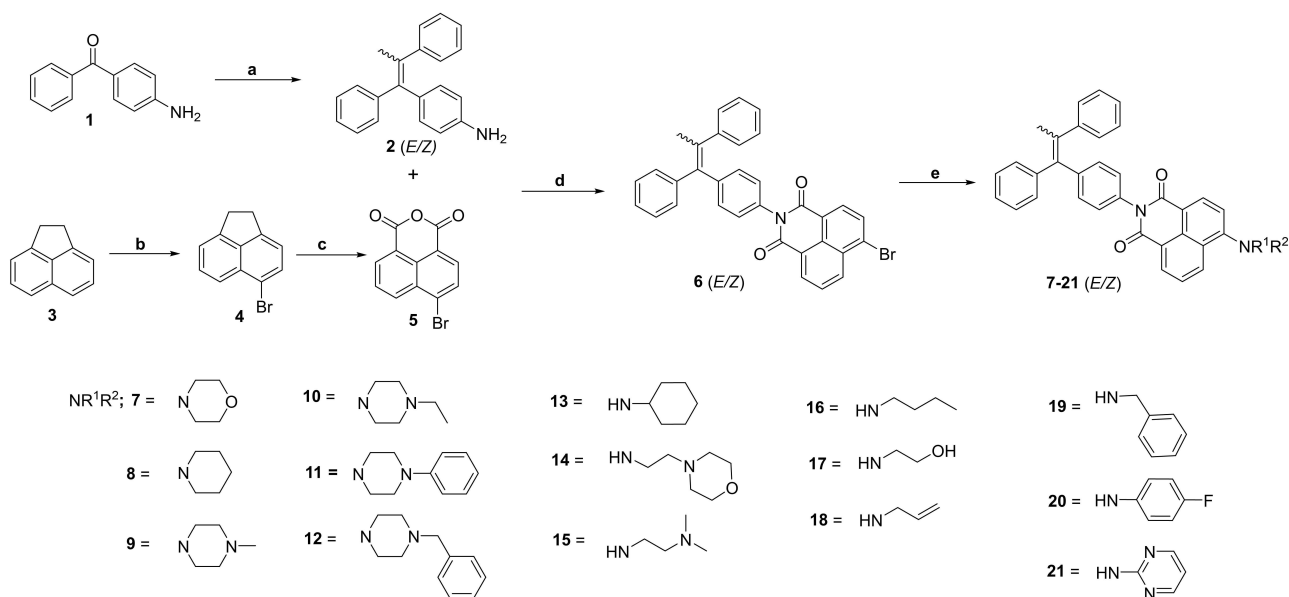
oisomerase inhibitors,<sup>[11,21]</sup> therefore herein, the mechanism of cytotoxicity of most potent TPE-naphthalimide **7** is elucidated through topoisomerase-II (TOPO-II) inhibition assay. Furthermore, molecular modeling was performed to determine the interactions between TOPO-II and TPE-naphthalimide which supports the plausible experimental data. The transportation behavior against most potent TPE-naph conjugate with human serum albumin (HSA) has also been explored with spectroscopy techniques.

## Results and Discussion

Triphenylethylene-naphthalimide conjugates were synthesized *via* multistep reactions including molecular hybridization technique (Scheme 1). Initially, McMurry reaction<sup>[23]</sup> was employed using the precursors 4-aminobenzophenone (**1**) and acetophenone in the presence of Zn and TiCl<sub>4</sub> in anhydrous THF to afford 4-(1,2-diphenylprop-1-en-1-yl)aniline (**2**) in 60% yield.

Subsequent treatment of acenaphthene (**3**) with *N*-bromosuccinimide in DMF at room temperature, furnished intermediate **4** in 97% yield. Further, oxidation of intermediate **4** was accomplished with refluxing of K<sub>2</sub>Cr<sub>2</sub>O<sub>7</sub> in acetic acid to afford 6-bromo-1*H*,3*H*-benzo[*de*]isochromene-1,3-dione (**5**) in 72% yield. 6-Bromo-2-(4-(1,2-diphenylprop-1-en-yl)phenyl)-1*H*-benzo[*de*]isoquinoline-1,3(2*H*)-dione (**6**) was obtained in quantitative yield on refluxing of compound **2** to a stirred solution of **5** in zinc acetate and ethanol for 15 h. Finally, compound **6** was refluxed with primary or secondary amine in the presence of potassium carbonate and DMF for 2–3 h to obtain isomeric products **7–21** in good yields. Attempts were made to separate *E* and *Z* isomers from mixture by column and preparative chromatography but was unsuccessful. Without separation of *E* and *Z* isomers, these synthesized compounds were characterized by NMR and mass spectrometric methods. The structures of synthesized TPE-naph were assigned on the basis of spectral data (Figures S1–S34 in the Supporting Information). For instance, <sup>1</sup>H NMR of conjugate **7** showed two characteristic multiplets (due to mixture of *E* and *Z* isomers) of morpholine at δ 4.04–3.99 and 3.29–3.24 ppm. The signals at δ values 67.0 and 53.5 ppm in <sup>13</sup>C NMR further confirmed the assigned structure.

To confirm the ratio and stereochemical assignment of *E* and *Z* configuration of TPE-naphthalimide conjugate **7**, reversed-phase high performance liquid chromatography (RP-HPLC) has been performed. Figure S35 represents the HPLC separation of *E* and *Z* isomers of analogue **7** with retention times 15.77 and 17.42 min, respectively. Further, *E/Z* ratio of TPE-naph was determined by <sup>1</sup>H NMR from the respective integral of methyl protons.<sup>[24]</sup> <sup>1</sup>H NMR spectrum of compound **7** (*E/Z*) exhibited two methyl singlets centered at 2.21 and 2.15 ppm. The singlets at δ values 2.21 and 2.15 ppm are due to CH<sub>3</sub> group, which was assigned *E* (*t<sub>r</sub>* = 15.77 min) and *Z* configurations (*t<sub>r</sub>* = 17.42 min), respectively. The signal identities were established on the basis of retention times of compound **7** obtained from chromatogram. As well the ratios of *E* and *Z*



**Scheme 1.** Synthesis of triphenylethylene-naphthalimide conjugates. a) Zn,  $TiCl_4$ , acetophenone, pyridine, THF,  $N_2$ , 0 °C to reflux, 60% yield; b) N-bromosuccinimide, DMF, RT, 3 h, 97% yield; c)  $K_2Cr_2O_7$ , acetic acid, reflux, 4 h, 72% yield; d)  $Zn(OAc)_2$ , EtOH, reflux, 15 h, 98% yield; e)  $HNR^1R^2$ ,  $K_2CO_3$ , DMF, reflux, 2–3 h, 60–80% yields.

isomers of analogue 7 were calculated from  $^1H$  NMR is same as that found from HPLC methodology, that is, 1:3.3. Moreover, the stereochemical assignments of *E* and *Z* configurations were given on the basis of NOESY spectroscopy (Figure S36). It has been observed that methyl signal at 2.15 ppm (*Z* isomer) interacts with the protons of alpha phenyl ring, which are shielded, that is, at  $\delta$  value 7.23 ppm. Therefore, it is concluded that protons of *E* isomer of TPE-naphthalimide conjugate were found to be deshielded than *Z* isomer and this relationship also holds good for tamoxifen.<sup>[25,26]</sup>

## Anti-proliferative activity

Preliminary, *in vitro* antiproliferative activity of compounds (*E/Z*) 7–21 at single dose concentration (10  $\mu$ M) was evaluated against 60 human cancer cell lines by National Cancer Institute (NCI, Bethesda, USA; Figure S37).<sup>[27]</sup> Among tested compounds, derivative 7 possessing morpholine group displayed excellent percentage growth inhibition against almost all cancer cell lines. Compound 7 exhibited good cytotoxicity towards non-small cell lung (HOP-92, GI = 78.7%; NCI-H23, GI = 78.4%), CNS (SF-295, GI = 71.5%) and ovarian (OVCAR-3, GI = 75.1%) cancer cell lines (Figure 3). It was inferred that compound 7 elicited improve cytotoxic potency towards NCI-H23 non-small cell lung), OVCAR-3 (ovarian) and MDA-MB-231 (breast cancer) cell lines in comparison to amonafide. When morpholinyl group of analogue 7 was replaced with piperidine moiety, it led to compound 8 with complete loss of antiproliferative activity which indicated that increase in lipophilicity reduces cytotoxicity towards cancer cell lines. Compound 9 (GI = –9.19%) with methyl piperazine moiety was found to be potent against SR

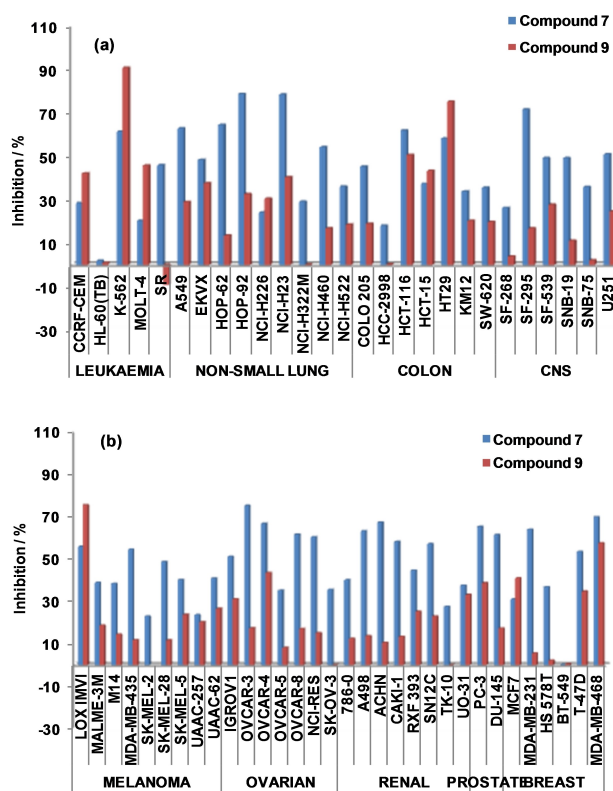


**Figure 3.** Comparison of anticancer activity between compound 7 and 9 against an *in vitro* panel of a) leukemia, non-small cell lung, colon, CNS cancer cell lines and b) melanoma, ovarian, renal, prostate, breast cancer cell lines.

leukemia cancer cell line when compared to amonafide (GI = 91.9%). Analogue 9 also exerted excellent anticancer activity

towards K-562 (leukemia cancer) cell line with growth inhibition of 90.8% (Figure 3). It has also been observed that compound **10** substituted with *N*-ethyl piperazinyl group showed lower activity when compared to **9** having *N*-methylpiperazinyl substituent that also proved that cytotoxicity is dependent upon lipophilicity. Derivative **11** (*N*-phenyl piperazine) displayed weak anticancer activity with average percentage of inhibition <40% except UO-31 (renal cancer) cell line while derivative belonging to *N*-benzyl piperazine (**12**) did not show any significant inhibition due to the presence of bulky amine.

On the other hand, compounds **13** (cyclohexyl amine), **15** (*N,N*-dimethyl ethylene diamine) and **17** (ethanol amine) with primary amines were least effective against cancer cell lines. Compound **14** bearing 4-(2-aminoethylene)morpholine was found to be sensitive towards leukemia (K-562, MOLT-4, RPMI-8226, SR), non-small cell lung (EKVX), colon (HCT-116, HCT-15), ovarian (OVCAR-4) and breast (MCF-7, T-47D) cancer cell lines with GI > 50%. Analogues **16** (GI = 40.4%) and **18** (GI = 45.4%) with respective butyl amine and allyl amine displayed selectivity towards UO-31 renal cancer cell line. Among derivatives **19**, **20** and **21** substituted with aromatic amines, only analogue **20** with 4-fluoroaniline showed significant activity against leukemia cancer cell line (K-562, GI = 67.9%; SR, GI = 63.1%) and colon cancer cell lines (HCT-15, GI = 52.9%; HT-29, GI = 61.4%). This might be attributed to the presence of fluoro at *para*-position of aniline. Thus, TPE-naph conjugates with secondary amines displayed promising percentage growth inhibition than analogues bearing primary amines. It was inferred that in this series **7–21**, compounds were found to be more sensitive towards leukemia and colon cancer cell lines. Moreover, from structure-activity relationship, it is demonstrated that increasing lipophilicity and bulkiness of substituent attached to C-4 position of naphthalimide ring resulted in decrease in cytotoxic activity. Therefore, the nature and size of amine influenced the anticancer activity of TPE-naph conjugates.

## Topoisomerase inhibition

Topoisomerase-II plays a key role in the segregation of strands of dsDNA which leads to replication resulting in proliferation of cell.<sup>[28]</sup> Therefore, to evaluate the mechanism of cytotoxicity of TPE-naph conjugates, we targeted the inhibitory effect of analogue **7** on topoisomerase-II $\alpha$  using supercoiled pHOT1 plasmid DNA. Etoposide, a well-known DNA intercalator was used as a positive control at 100  $\mu$ M. Figure 4 represents the inhibitory effect of **7** on the relaxation of plasmid DNA mediated by TOPO-II $\alpha$  at three different concentrations, that is, 25, 50 and 100  $\mu$ M. Compound **7** induces partial inhibitory activity at 25  $\mu$ M and complete inhibition at 50 and 100  $\mu$ M. It revealed that the inhibiting of TOPO-II by compound **7** suggested a possible mechanism of cytotoxicity through topoisomerase-II inhibition.

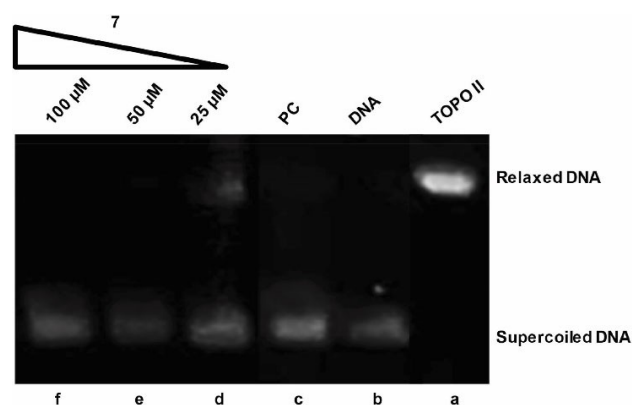


**Figure 4.** Effect of TPE-naph **7** on the relaxation of supercoiled plasmid DNA topoisomerase-II. Supercoiled DNA (lane b) was incubated with topoisomerase II in the absence (lane a) and presence of analogue **7** at 25  $\mu$ M (lane d), 50  $\mu$ M (lane e) and 100  $\mu$ M (lane f). Etoposide was used as positive control at 100  $\mu$ M (lane c).

## Human serum albumin studies

HSA is a major extracellular plasma protein in blood and featuring specific binding site for transportation and deposition of drug. The binding behavior of drug towards HSA could modulate its key pharmacodynamic and pharmacokinetic properties like efficacy, metabolism and drug distribution.<sup>[29]</sup> Various promising drugs due to their high binding affinity towards HSA were found to be futile. Henceforth, the binding interaction studies have been done between HSA and the biological active molecules insights drug-likeness properties as well as explore screening of molecules in drug discovery. Thus, to analyze the interaction between most active TPE-naph **7** and HSA, *in vitro* studies were carried out by UV-visible absorption and fluorescence emission techniques.

## UV-visible absorption spectroscopy

UV-visible spectroscopy is a reliable tool employed to determine the structural alterations in protein and to investigate the formation of complex on drug binding. In this study, absorption band of HSA at 280 nm (7  $\mu$ M) was recorded in phosphate buffer (0.1 M) at pH 7.4. The band at 280 nm corresponds to aromatic ring of amino acid residues Trp214, Tyr411 and Phe403 in HSA. On incremental addition of compound **7**, the enhancement in absorption band of HSA was observed with appearance of a new band at 400 nm (Figure 5a). The maximum peak of absorption remains unaltered which indicated that analogue **7** binds with the cavity of HSA through noncovalent interactions. This is evident by the existence of  $\pi$ - $\pi$  stacking interactions between the aromatic rings of analogue **7** and tryptophan, tyrosine and phenylalanine residues in the binding cavity of HSA.<sup>[30]</sup>

In order to evaluate the binding affinity of TPE-naph with HSA, the binding constant ( $K_b$ ) was calculated from a plot of  $1/(A-A_0)$  versus  $1/Q$  using Benesi-Hildebrand equation ( $1, S1$ )<sup>[31]</sup> and

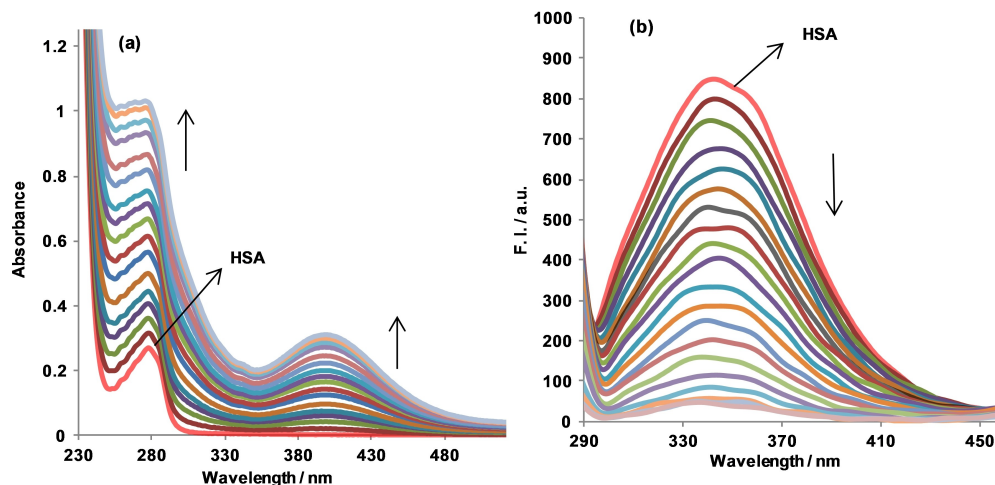


Figure 5. Effect of the incremental addition of analogue 7 on a) UV/Vis absorption and b) fluorescence emission of HSA (7  $\mu\text{M}$ ) in phosphate buffer (pH 7.4).

the ratio of intercept to slope was found to be equal to  $1.4 \times 10^4 \text{ M}^{-1}$  (Figure S38).

## Fluorescence spectroscopy

Fluorescence spectroscopy is a sophisticated technique which explores the binding interactions of drug and protein. Under physiological conditions, the fluorescence spectrum of HSA of 7 in phosphate buffer (pH 7.4) was recorded with an excitation wavelength of 280 nm. The fluorescence spectrum of HSA exhibited an emission band at 340 nm due to tryptophan residues. With incremental addition of compound 7, the emission band of HSA at 340 nm was consistently quenched which revealed some changes around Trp214 of HSA (Figure 5b). The  $\lambda_{\text{max}}$  of emission of HSA displayed hypsochromic shift by 5 nm (from 340 to 335 nm). This indicated that analogue 7 interacts with the hydrophobic cavity of HSA.

The quenching of emission band of HSA upon incremental addition of 7 is the result of either dynamic or static quenching. Further, the Stern-Volmer equation (S2) was employed to evaluate Stern-Volmer constant,  $K_{\text{SV}}$  and the bimolecular collision constant,  $K_{\text{q}}$  which explicate the binding mode of 7 to HSA.<sup>[32]</sup> (Figure S39). From the linear plot of regression curve of  $F_0/F$  versus  $[Q]$ ,  $K_{\text{SV}}$  and  $K_{\text{q}}$  were calculated to be  $6.8 \times 10^4 \text{ M}^{-1}$  and  $1.6 \times 10^{13} \text{ M}^{-1} \text{ s}^{-1}$ , respectively. As the bimolecular collision constant ( $K_{\text{q}}$ ) for HSA:TPE-naph system is greater than diffusion limiting quenching in water,<sup>[33]</sup> that is,  $2 \times 10^{10} \text{ M}^{-1} \text{ s}^{-1}$  which suggested the nature of quenching in the present case is static, that is, formation of analogue 7 and HSA complex in ground state.<sup>[34]</sup> Further, the binding constant and the number of binding sites have been determined using a modified Stern-Volmer equation (S3) from the plot of  $\log [(F_0 - F)/F]$  versus  $\log [Q]$  which give  $K_{\text{b}}$  and  $n$  as intercept and slope, respectively.<sup>[35]</sup> The binding constant of compound 7 toward HSA was calculated to be  $1.4 \times 10^4 \text{ M}^{-1}$  and the number of binding sites per HSA was

nearly one that revealed strong binding interaction among HSA and TPE-naph (Figure S40).

To determine the spontaneity for formation of complex between conjugate 7 and HSA, change in free energy has been calculated that was found to be  $-8.4 \text{ kcal/mol}$  by employing following equation 1.<sup>[36]</sup> The negative value of  $\Delta G$  demonstrates spontaneity and existence of hydrophobic interaction among HSA:TPE-naph.

$$\Delta G = -RT \ln K_{\text{b}} \quad (1)$$

## Life-time fluorescence technique

The quenching of HSA emission by TPE-naph is either due to static quenching or dynamic quenching mechanism. In order to have better understanding of quenching mechanism, time-resolved fluorescence experiment was carried out.<sup>[37]</sup> Figure 6

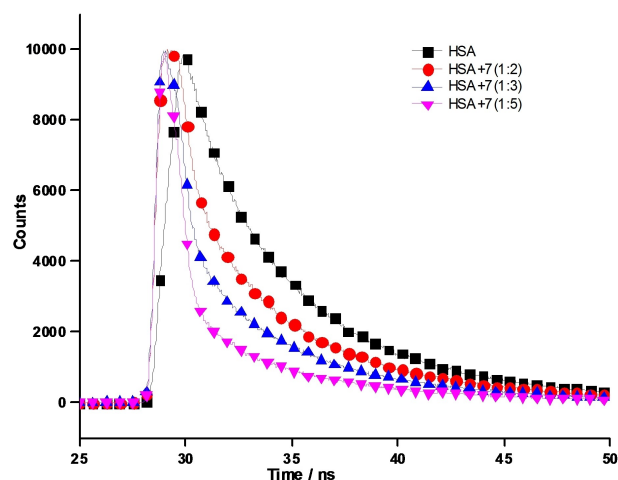


Figure 6. Fluorescence decay profile of HSA on addition of various concentrations of 7 in phosphate buffer (pH 7.4).

**Table 1.** Fluorescence decay profile of HSA and compound 7.

System	Conc.	$\tau_1$ [ns]	$\tau_2$ [ns]	$\tau_3$ [ns]	$\alpha_1$	$\alpha_2$	$\alpha_3$	$\tau_{av}$	$\chi^2$
HSA		3.64	6.97	1.17	0.26	0.70	0.02	5.06	1.01
HSA-7	1:2	3.65	7.47	0.51	0.35	0.60	0.04	4.80	1.11
	1:3	4.19	7.94	0.64	0.42	0.45	0.12	4.10	1.39
	1:5	3.47	7.83	0.43	0.32	0.53	0.13	2.11	1.23

represents the life-time decay profile of HSA (7  $\mu$ M) in the absence and presence of different concentrations of compound 7. The average lifetime triexponential values were calculated using the equation 2. Upon addition of 14  $\mu$ M of analogue 7, the life-time of HSA decrease is marginal (5.06 to 4.80 ns). As depicted from Table 1, at higher concentration (21–35  $\mu$ M) of conjugate 7, reduction in lifetime of HSA is more pronounced. It revealed that other phenomena of quenching may also exist i.e. dynamic quenching. While the steady state fluorescence experiment demonstrate the possibility of static quenching. From above results, it was inferred that both the static as well as dynamic quenching might be responsible for the interaction of analogue 7 to HSA.

$$\tau_{av} = \alpha_1\tau_1 + \alpha_2\tau_2 + \alpha_3\tau_3 \quad (2)$$

## Molecular docking studies

To better understand the inhibition behavior of *E* and *Z* isomers of TPE-naph analogue 7 towards TOPO-II-DNA complex (PDB ID: 5GWK), docking studies have been performed using AutoDock vina 4.0 software.<sup>[38]</sup> From docking studies, the binding energy scores *E* and *Z* isomers for analogue 7 and reference drug etoposide were calculated to be –11.3, –11.3 and –9.8 kcal/mol, respectively. It was observed that *E* and *Z* isomers of conjugate 7 exhibited better binding affinity than reference drug etoposide while these binds only with amino acid residues of TOPO-II. It demonstrates the existence of strong intermolecular forces between the ligands and TOPO-II. Figure 7 represents the 3D docked structures of compound 7 (*E* isomer, a; *Z* isomer, b) and etoposide with TOPO-II-DNA complex. From the binding pattern, it was inferred that *E* isomer of 7 interacts with the active sites of TOPO-II-DNA complex via THR618 ( $d=2.23$  Å) through conventional-hydrogen bonding; TYR805, LYS611, LYS614 and PHE807 residues through alkyl-alkyl and  $\pi$ -alkyl hydrophobic interactions while *Z*-isomer of analogue 7 showed unconventional hydrogen bonding (Asp541, Tyr805) and hydrophobic interactions, (Gly617, Thr618, Lys614 and Phe807). On the other hand, etoposide binds with TOPO-II complex through Asn770 ( $d=2.38$  Å) and Gln773 ( $d=2.52$  Å) residues by conventional hydrogen bondings; Met766 through hydrophobic interactions; and sugar backbone of DNA through DT-5 ( $d=2.82$  Å), DC-4 ( $d=3.75$  Å), DA-6 ( $d=2.95$  Å), DG-5 ( $d=3.10$  Å). The results of docking studies are consistent with our experimental data and proved that TPE-naphthalimide conjugate acts as TOPO-II inhibitor.

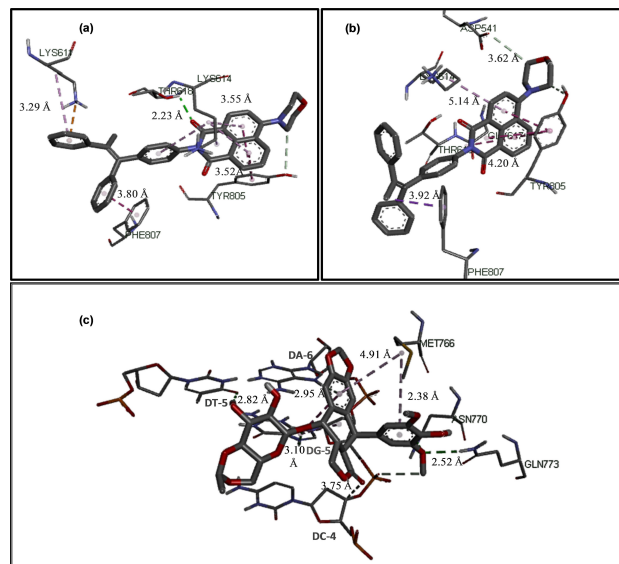


**Figure 7.** 3D docked structures of compound 7. a) *E* isomer, b) *Z* isomer and c) etoposide with topoisomerase-II-DNA complex (PDB ID: 5GWK).

## Conclusion

A novel series of triphenylethylene-naphthalimide conjugates has been synthesized by substituting different amines at the C-4 position of naphthalimide ring and evaluated for their cytotoxicity towards 60 human cancer cell lines. Preliminary results indicated that TPE-naph conjugates were found to be more sensitive towards leukemia and colon subpanels at one-dose concentration (10  $\mu$ M). Among synthesized analogues, only compound 7 bearing morpholinyl group exhibited excellent broad-spectrum activity. It was also observed that an increase in the lipophilicity of the substituent lowers the cytotoxicity of TPE-naph hybrids towards cancer cell lines. More importantly, it is concluded that TPE-naph derivatives substituted with secondary amines exhibited better cytotoxicity. Thus, SAR studies revealed that the nature and bulkiness of substituent play key roles in antiproliferative activity of TPE-naph. The most active compound, 7, significantly inhibited the activity of TOPO-II at 50  $\mu$ M concentration. This suggested the plausible mechanism of cytotoxicity through TOPO-II inhibition; also supported by docking results. The docking results analyzed the preferential binding sites of TPE-conjugate 7 with the TOPO-II-DNA complex. It was observed that the oxygen atoms of naphthalimide and phenyl rings of triphenylethylene interacts only with TOPO-II through hydrogen bonding and  $\pi$ - $\pi$  stacking hydrophobic forces with binding affinity –11.3 kcal/

mol. Unlike etoposide, TPE-naph conjugate **7** interacts only with TOPO-II. Thus, it indicated TPE-naph conjugate act as TOPO-II inhibitor. Moreover, the interaction of **7** with HSA indicated the binding constant in order of  $10^4 \text{ M}^{-1}$  which is the evident of drug-likeness properties of these analogues. Thus, the present manuscript highlights the approaches employed to design and synthesize new molecular framework (triphenylethylene-naphthalimide conjugates) as therapeutic template to target TOPO-IIa for anticancer activity. These results extended a new route to design and develop efficient drug candidates as anticancer agent.

## Experimental Section

### Reagents and conditions

All the chemicals and reagents were commercially available from Spectrochem, Aldrich (Sigma-Aldrich), TCI and used without further purification. Analytical TLC was performed using spectrochem silica gel (GF-254) pre-coated plates and visualized TLC under UV light or by iodine indicator.  $^1\text{H}$  NMR spectra were carried out on Jeol spectrometer 400 MHz and Bruker –500 MHz while  $^{13}\text{C}$  NMR spectra were recorded on Jeol spectrometer 100 MHz, using deuterated solvents ( $\text{CDCl}_3$  and  $[\text{D}_6]\text{DMSO}$ ). Using TMS as an internal reference, chemical shifts ( $\delta$ ) and coupling constants ( $J$ ) were recorded in ppm and Hz, respectively. Melting points were determined on equiptronics melting point apparatus and were uncorrected. UV/Vis and fluorescence studies were accomplished on Shimadzu and Varian Cary Eclipse fluorescence spectrophotometer, respectively. The time fluorescence studies were carried out using deltaflex™ spectrometer. Mass spectra of synthesized compounds were observed at water Micromass-Q-T of Micro.

### Synthesis

**4-(1,2-Diphenylprop-1-en-1-yl)aniline (2):** Titanium tetrachloride (2.77 mL, 25.30 mmol) was added gradually to a suspension of Zn (3.24 g, 50.75 mmol) in dry THF (40 mL) under the atmosphere of nitrogen at  $0^\circ\text{C}$ . Subsequently, the resulting black mixture was allowed to reflux for 3 h to produce titanium reagent. After refluxing, the obtained titanium reagent was cooled to  $0^\circ\text{C}$  and charged with pyridine (1.02 mL, 12.7 mmol). Then, a solution of acetophenone (0.59 mL, 5.07 mmol) and 4-amino benzophenone (1 g, 5.07 mmol) in THF was added dropwise to reaction mixture at  $0^\circ\text{C}$  and stirred for 30 min. The reaction mixture was heated to reflux for 2.5 h. The completion of reaction was monitored by TLC. On completion, 10% aq. soln. of  $\text{K}_2\text{CO}_3$  was poured into the cooled reaction mixture and stirred vigorously for 10 min. On stirring, a black mass was separated out that removed by vacuum filtration. The crude product was extracted from the filtrate with ethyl acetate. The extracted organic layer was dried over  $\text{Na}_2\text{SO}_4$  and the solvent was evaporated. Further, the resulting brownish-yellow oil was purified by column chromatography (hexane/ethylacetate 97:3) to provide a desired cross-coupled product (**2**) in diastereomeric isomers *E/Z* 1:6; yield 60%; mp: 142–144  $^\circ\text{C}$ ;  $^1\text{H}$  NMR (400 MHz,  $\text{CDCl}_3$ ):  $\delta$  = 7.35–7.32 (m, 2H, ArH), 7.26–7.23 (m, 3H, ArH), 7.17 (brs, 3H, ArH), 7.13–7.09 (m, 2H, ArH), 7.04–6.96 (m, 1H, ArH), 6.91–6.88 (m, 1H, ArH), 6.67–6.65 (m, 2H, ArH), 6.36–6.33 (m, 2H, ArH), 3.48 (s, 2H,  $\text{NH}_2$ ), 2.18 (s, 3H,  $\text{CH}_3$ ), 2.10 (s, 3H,  $\text{CH}_3$ );  $^{13}\text{C}$  NMR (100 MHz,  $\text{CDCl}_3$ ):  $\delta$  = 144.6, 144.2, 144.1, 144.0, 139.1, 134.1, 134.0, 133.6, 132.2, 130.1, 129.5, 129.4, 128.1, 127.9, 127.8, 126.5, 126.0, 114.3 (ArC), 23.4 ( $\text{CH}_3$ ); ESIMS: *m/z* 286.2 ( $\text{M} + \text{H}$ ) $^+$ .

**5-Bromo-1,2-dihydroacenaphthylene (4):**<sup>[39]</sup> To a suspension of acenaphthene (3 g, 19.4 mmol) in DMF, a solution of *N*-bromosuccinimide (4.15 g, 23.35 mmol) in 30 mL of DMF was added slowly at room temperature. The solution was stirred vigorously for 3 h. The reaction was quenched by adding 300 mL of cold water into solution, and brown colored precipitates were obtained on filtration. The crude was recrystallized to obtain pure 5-bromo-1,2-dihydroacenaphthylene (**4**) in 97% yield (mp: 54–56  $^\circ\text{C}$ ).

**4-Bromo-1,8-naphthalic anhydride (5):**<sup>[40]</sup> Potassium dichromate (6.31 g, 21.45 mmol) was added slowly to a solution of 5-bromo acenaphthene **4** (1 g, 4.2 mmol) in glacial acetic acid at  $0^\circ\text{C}$ . The mixture was stirred for 10 min at room temperature and then allowed to reflux for 4 h. The cooled reaction mixture was poured into 500 mL of water and filtered to provide green colored precipitates. The excess chromium salt left in residue was removed by washing with boiled water. After washing, white colored solid (**5**) was obtained in 72% yield (mp: 221–224  $^\circ\text{C}$ ).

**6-Bromo-2-(4-(1,2-diphenylprop-1-en-1-yl)phenyl)-1H-benzo[de]isoquinoline-1,3(2H)-dione (6):** To a two necked round-bottom flask, 4-bromo-1,8-naphthalic anhydride (**5**; 1 g, 3.61 mmol) and zinc acetate (0.95 g, 4.3 mmol) were dispersed in 15 mL of ethanol under the inert atmosphere. To the stirred reaction mixture, 4-(1,2-diphenylprop-1-en-1-yl)aniline (**2**) (0.52 g, 1.81 mmol) was added and heated to reflux for 15 h. After completion of reaction, the hot filtration of the suspension was carried out and repeatedly washed with ethanol. The crude was purified by column chromatography (hexane/chloroform 8:2) to obtain a yellow colored pure product (**6**) in 98% yield; *E/Z* 1:2;  $^1\text{H}$  NMR (400 MHz,  $\text{CDCl}_3$ ):  $\delta$  = 8.67–8.64 (m, 1H, ArH), 8.62–8.59 (m, 2H, ArH), 8.44–8.42 (d,  $J$  = 7.88 Hz, 1H, ArH), 8.37–8.35 (d,  $J$  = 7.88 Hz, 1H, ArH), 8.14–8.12 (d,  $J$  = 7.92 Hz, 1H, ArH), 8.10–8.08 (d,  $J$  = 7.92 Hz, 1H, ArH), 7.97–7.89 (m, 2H, ArH), 7.43–7.37 (m, 4H, ArH), 7.31–7.29 (d,  $J$  = 7.96 Hz, 4H, ArH), 7.23–7.22 (m, 2H, ArH), 7.16–7.10 (m, 4H, ArH), 7.08–7.02 (m, 4H, ArH), 6.97–6.95 (m, 3H, ArH), 2.21 (s, 3H,  $\text{CH}_3$ ), 2.13 (s, 3H,  $\text{CH}_3$ );  $^{13}\text{C}$  NMR (100 MHz,  $\text{CDCl}_3$  +  $[\text{D}_6]\text{DMSO}$ ):  $\delta$  = 163.7, 163.6, 163.5, 143.7, 143.6, 143.5, 143.2, 143.1, 142.7, 138.4, 138.3, 136.6, 136.5, 133.7, 133.6, 132.8, 132.3, 132.2, 131.5, 131.4, 131.3, 131.2, 130.8, 130.7, 130.6, 130.5, 130.0, 129.9, 129.3, 129.2, 128.5, 128.4, 128.3, 128.1, 127.9, 127.7, 127.6, 126.8, 126.6, 123.3, 123.2, 122.4, 122.3 (ArC), 23.6 ( $\text{CH}_3$ ), 23.5 ( $\text{CH}_3$ ); ESI MS: *m/z* 544.0 ( $\text{M} + \text{H}$ ) $^+$ .

**6-Amino substituted-2-(4-(1,2-diphenylprop-1-en-1-yl)phenyl)-1H-benzo[de]isoquinoline-1,3(2H)-diones (7–21):** A mixture of 6-bromo-2-(4-(1,2-diphenylprop-1-en-1-yl)-1H-benzo[de]isoquinoline-1,3(2H)-dione (**6**) (0.2 g, 0.37 mmol) and corresponding primary or secondary amine (1.1 mmol) was refluxed for 2–3 h in the presence of potassium carbonate (0.06 g, 0.44 mmol) in 10 mL of DMF. The reaction mixture was allowed to cool and poured in water (50 mL) to obtain precipitates. Then, the mixture was filtered off to get corresponding solid crude product of 6-amino substituted-2-(4-(1,2-diphenylprop-1-en-1-yl)-1H-benzo[de]isoquinoline-1,3(2H)-diones (7–21) which was purified by column chromatography over silica gel using hexane and chloroform as eluents.

**2-(4-(1,2-Diphenylprop-1-en-1-yl)phenyl)-6-morpholino-1H-benzo[de]isoquinoline-1,3(2H)-dione (7):** Yellow solid, *E/Z* 1:3.3; Yield 77%; mp: 236–240  $^\circ\text{C}$ ;  $^1\text{H}$  NMR (400 MHz,  $\text{CDCl}_3$ ):  $\delta$  = 8.63–8.61 (dd, 1H,  $^2J$  = 7.28 Hz,  $^3J$  = 0.92 Hz, ArH), 8.58–8.55 (m, 1H, ArH), 8.51–8.49 (d, 1H,  $J$  = 8.00 Hz, ArH), 8.48–8.45 (m, 1H, ArH), 8.44–8.41 (m, 1H, ArH), 7.76–7.74 (m, 1H, ArH), 7.72–7.68 (m, 1H, ArH), 7.41–7.34 (m, 3H, ArH), 7.30–7.25 (m, 4H, ArH), 7.23–7.21 (m, 5H, ArH), 7.16–7.11 (m, 2H, ArH), 7.03–7.00 (m, 3H, ArH), 6.95–6.92 (m, 3H, ArH), 4.04–3.99 (m, 5H, morph-OCH $_2$ ), 3.29–3.24 (m, 5H, morph-NCH $_2$ ), 2.21 (s, 1H,  $\text{CH}_3$ ), 2.15 (s, 3H,  $\text{CH}_3$ );  $^{13}\text{C}$  NMR (100 MHz,  $\text{CDCl}_3$ ):  $\delta$  = 164.7, 164.5, 164.2, 164.1, 156.0, 155.9, 144.0, 143.7, 143.3, 143.1, 142.8, 138.7, 138.6, 136.5, 136.4, 133.1, 133.0, 132.9, 131.7, 131.5, 131.1,

131.0, 130.5, 130.4, 130.3, 129.4, 128.5, 128.3, 128.2, 127.9, 127.6, 127.5, 126.7, 126.6, 126.3, 126.2, 126.1, 126.0, 123.5, 117.2, 115.2, 115.1 (ArC), 67.0 (morph-OCH<sub>3</sub>), 53.5 (morph-NCH<sub>3</sub>), 23.6 (CH<sub>3</sub>), 22.9 (CH<sub>3</sub>); HRMS (TOF MS): *m/z* calcd C<sub>37</sub>H<sub>30</sub>N<sub>2</sub>O<sub>3</sub> 551.2256, found 551.2230.

**2-(4-(1,2-Diphenylprop-1-en-1-yl)phenyl)-6-(piperidin-1-yl)-1H-benzo[de]isoquinoline-1,3(2H)-dione (8):** Yellow solid, *E/Z* 1:2.2; Yield 72%; mp: 235–238 °C; <sup>1</sup>H NMR (400 MHz, CDCl<sub>3</sub>): δ = 8.61–8.59 (m, 1H, ArH), 8.54–8.51 (m, 1H, ArH), 8.47–8.45 (d, *J* = 7.28 Hz, 1H, ArH), 8.44–8.42 (m, 1H, ArH), 8.40–8.38 (m, 1H, ArH), 7.41–7.33 (m, 3H, ArH), 7.30–7.26 (m, 4H, ArH), 7.22–7.17 (m, 5H, ArH), 7.15–7.08 (m, 4H, ArH), 7.03–6.99 (m, 3H, ArH), 6.95–6.92 (m, 3H, ArH), 3.28–3.20 (m, 6H, pip-NCH<sub>2</sub>), 1.92–1.84 (m, 6H, pip-CH<sub>2</sub>), 1.76–1.70 (m, 3H, pip-CH<sub>2</sub>); <sup>13</sup>C NMR (100 MHz, CDCl<sub>3</sub>): δ = 163.9, 163.7, 163.4, 163.2, 156.7, 156.6, 143.0, 142.7, 142.5, 142.3, 142.0, 141.8, 137.7, 137.6, 135.4, 132.2, 132.0, 130.7, 130.5, 130.4, 130.1, 130.0, 129.4, 129.3, 128.4, 127.4, 127.2, 127.1, 126.9, 126.7, 126.5, 125.7, 125.6, 125.4, 125.0, 124.5, 124.4, 122.3, 114.9, 113.9, 113.8 (ArC), 53.6 (pip-NCH<sub>2</sub>), 28.7 (pip-CH<sub>2</sub>), 25.3 (pip-CH<sub>2</sub>), 23.4 (CH<sub>3</sub>), 22.6 (CH<sub>3</sub>); HRMS (TOF MS): *m/z* calcd C<sub>38</sub>H<sub>32</sub>N<sub>2</sub>O<sub>2</sub> 549.2464, found 549.2438.

**2-(4-(1,2-Diphenylprop-1-en-1-yl)phenyl)-6-(4-methylpiperazin-1-yl)-1H-benzo[de]isoquinoline-1,3(2H)-dione (9):** Yellow solid, *E/Z* 1:3.5; yield 78%; mp: 239–242 °C; <sup>1</sup>H NMR (400 MHz, CDCl<sub>3</sub>): δ = 8.62–8.60 (m, 1H, ArH), 8.56–8.54 (m, 1H, ArH), 8.49–8.47 (d, *J* = 8.08 Hz, 1H, ArH), 8.46–8.44 (m, 1H, ArH), 8.42–8.40 (m, 1H, ArH), 7.74–7.72 (m, 1H, ArH), 7.70–7.66 (m, 1H, ArH), 7.41–7.33 (m, 3H, ArH), 7.30–7.25 (m, 4H, ArH), 7.22–7.20 (m, 5H, ArH), 7.16–7.07 (m, 3H, ArH), 7.03–7.00 (m, 3H, ArH), 6.95–6.92 (m, 3H, ArH), 3.32–3.30 (m, 5H, pip-NCH<sub>2</sub>), 2.74–2.73 (m, 5H, pip-NCH<sub>2</sub>), 2.44 (s, 1H, pip-NCH<sub>3</sub>), 2.42 (s, 3H, pip-NCH<sub>3</sub>), 2.21 (s, 1H, CH<sub>3</sub>), 2.15 (s, 3H, CH<sub>3</sub>); <sup>13</sup>C NMR (100 MHz, CDCl<sub>3</sub> + [D<sub>6</sub>]DMSO): δ = 164.4, 163.9, 156.4, 156.3, 143.6, 143.2, 142.9, 138.4, 136.4, 131.3, 131.2, 130.8, 130.1, 130.0, 129.2, 128.3, 128.1, 127.8, 126.8, 126.6, 126.1, 125.7, 123.3, 123.2, 116.4, 116.3, 115.0 (ArC), 55.0 (pip-NCH<sub>2</sub>), 53.0 (pip-NCH<sub>2</sub>), 52.9 (pip-NCH<sub>2</sub>), 46.2 (NCH<sub>3</sub>), 46.1 (NCH<sub>3</sub>), 23.6 (CH<sub>3</sub>); HRMS (TOF MS): *m/z* calcd C<sub>38</sub>H<sub>33</sub>N<sub>3</sub>O<sub>2</sub> 564.2573, found 564.2546.

**2-(4-(1,2-Diphenylprop-1-en-1-yl)phenyl)-6-(4-ethylpiperazin-1-yl)-1H-benzo[de]isoquinoline-1,3(2H)-dione (10):** Yellow solid, *E/Z* 1:3.6; yield 74%; mp: 240–243 °C; <sup>1</sup>H NMR (400 MHz, CDCl<sub>3</sub>): δ = 8.62–8.57 (m, 1H, ArH), 8.55–8.53 (m, 1H, ArH), 8.49–8.46 (m, 1H, ArH), 8.44–8.40 (m, 1H, ArH), 8.24–8.22 (m, 1H, ArH), 7.77–7.71 (m, 1H, ArH), 7.69–7.65 (m, 1H, ArH), 7.40–7.33 (m, 3H, ArH), 7.30–7.26 (m, 4H, ArH), 7.22–7.19 (m, 5H, ArH), 7.15–7.09 (m, 2H, ArH), 7.04–6.99 (m, 3H, ArH), 6.98–6.92 (m, 3H, ArH), 3.31 (brs, 4H, pip-NCH<sub>2</sub>), 2.77 (brs, 4H, pip-NCH<sub>2</sub>), 2.60–2.53 (m, 3H, NCH<sub>2</sub>), 2.21 (s, 1H, CH<sub>3</sub>), 2.14 (s, 3H, CH<sub>3</sub>), 1.19–1.14 (m, 4H, NCH<sub>2</sub>); <sup>13</sup>C NMR (100 MHz, CDCl<sub>3</sub> + [D<sub>6</sub>]DMSO): δ = 164.5, 163.9, 156.3, 143.8, 143.6, 143.5, 143.3, 143.2, 142.9, 138.5, 138.4, 138.3, 136.5, 136.4, 133.2, 132.8, 131.5, 131.4, 131.3, 131.2, 130.9, 130.8, 130.6, 130.1, 130.0, 129.3, 129.2, 128.1, 127.9, 127.7, 127.5, 126.7, 126.5, 126.1, 125.7, 123.1, 116.3, 114.9 (ArC), 53.0 (pip-NCH<sub>2</sub>), 52.9 (pip-NCH<sub>2</sub>), 52.7 (ethyl-NCH<sub>2</sub>), 52.3 (pip-NCH<sub>2</sub>), 23.6 (CH<sub>3</sub>), 23.5 (CH<sub>3</sub>), 12.0 (ethyl-CH<sub>3</sub>); HRMS (TOF MS): *m/z* calcd C<sub>39</sub>H<sub>35</sub>N<sub>3</sub>O<sub>2</sub> 578.2729, found 578.2800.

**2-(4-(1,2-Diphenylprop-1-en-1-yl)phenyl)-6-(4-phenylpiperazin-1-yl)-1H-benzo[de]isoquinoline-1,3(2H)-dione (11):** Yellow solid, *E/Z* 1:1; Yield 79%; mp: 245–248 °C; <sup>1</sup>H NMR (500 MHz, CDCl<sub>3</sub>): δ = 8.66–8.64 (d, *J* = 7.25 Hz, 1H, ArH), 8.60–8.58 (m, 2H, ArH), 8.54–8.52 (d, *J* = 7.85 Hz, 2H, ArH), 8.50–8.48 (d, *J* = 8.40 Hz, 1H, ArH), 7.78–7.71 (m, 2H, ArH), 7.43–7.41 (d, *J* = 8.35 Hz, 2H, ArH), 7.39–7.28 (m, 15H, ArH), 7.24–7.21 (m, 4H, ArH), 7.17–7.16 (m, 4H, ArH), 7.13–7.10 (m, 1H, ArH), 7.06–7.03 (m, 8H, ArH), 6.96–6.92 (m, 6H, ArH), 3.55–3.50 (m, 8H, pip-NCH<sub>2</sub>), 3.48–3.44 (m, 8H, pip-NCH<sub>2</sub>), 2.23 (s, 3H, CH<sub>3</sub>), 2.17 (s, 3H, CH<sub>3</sub>); <sup>13</sup>C NMR (100 MHz, CDCl<sub>3</sub>): δ = 164.7, 164.6, 164.3, 164.1, 156.1, 156.0, 151.1, 143.7, 143.6, 143.3, 143.1, 142.8, 138.6,

136.5, 132.9, 131.7, 131.5, 131.1, 131.0, 130.3, 130.2, 129.4, 129.3, 128.2, 128.1, 127.9, 127.7, 126.7, 126.6, 126.4, 126.3, 126.1, 126.0, 125.9, 123.6, 123.5, 120.5, 117.2, 117.1, 116.6, 116.5, 115.2 (ArC), 53.2 (pip-NCH<sub>2</sub>), 53.1 (pip-NCH<sub>2</sub>), 49.7 (pip-NCH<sub>2</sub>), 49.6 (pip-NCH<sub>2</sub>), 23.7 (CH<sub>3</sub>), 23.6 (CH<sub>3</sub>); HRMS (TOF MS): *m/z* calcd C<sub>43</sub>H<sub>35</sub>N<sub>3</sub>O<sub>2</sub> 626.2729, found 626.2709.

**6-(4-Benzylpiperazin-1-yl)-2-(4-(1,2-diphenylprop-1-en-1-yl)phenyl)-1H-benzo[de]isoquinoline-1,3(2H)-dione (12):** Yellow solid, *E/Z* 1:1.4; Yield 75%; mp: 246–249 °C; <sup>1</sup>H NMR (400 MHz, CDCl<sub>3</sub>): δ 8.62–8.60 (d, *J* = 7.2 Hz, 1H, ArH), 8.55–8.53 (d, *J* = 7.80 Hz, 2H, ArH), 8.49–8.40 (m, 3H, ArH), 7.72–7.64 (m, 2H, ArH), 7.41–7.32 (m, 11H, ArH), 7.31–7.22 (m, 10H, ArH), 7.18–7.14 (m, 5H, ArH), 7.11–7.07 (m, 2H, ArH), 7.05–7.00 (m, 5H, ArH), 6.95–6.92 (m, 4H, ArH), 3.67 (s, 2H, benzyl-CH<sub>2</sub>), 3.65 (s, 2H, benzyl-CH<sub>2</sub>), 3.32–3.29 (m, 7H, pip-NCH<sub>2</sub>), 2.78 (brs, 7H, pip-NCH<sub>2</sub>), 2.22 (s, 3H, CH<sub>3</sub>), 2.15 (s, 3H, CH<sub>3</sub>); <sup>13</sup>C NMR (100 MHz, CDCl<sub>3</sub>): δ = 164.8, 164.6, 164.3, 164.1, 144.1, 144.0, 143.7, 143.6, 143.3, 143.1, 142.8, 140.0, 138.8, 138.7, 138.6, 138.0, 136.4, 133.1, 133.0, 132.9, 131.8, 131.7, 131.6, 131.4, 131.1, 130.9, 130.7, 130.6, 130.3, 130.2, 129.4, 129.3, 128.5, 128.4, 128.2, 128.1, 127.9, 127.7, 127.5, 127.4, 126.7, 126.6, 126.3, 126.2, 125.9, 125.8, 125.8, 123.4 (ArC), 65.4 (benzyl CH<sub>2</sub>), 65.3 (benzyl CH<sub>2</sub>), 53.2 (pip-CH<sub>2</sub>), 53.1 (pip-CH<sub>2</sub>), 53.0 (pip-CH<sub>2</sub>), 23.7 (CH<sub>3</sub>), 23.6 (CH<sub>3</sub>); HRMS (TOF MS): *m/z* calcd C<sub>44</sub>H<sub>37</sub>N<sub>3</sub>O<sub>2</sub> 640.2886, found 640.2860.

**6-(Cyclohexylamino)-2-(4-(1,2-diphenylprop-1-en-1-yl)phenyl)-1H-benzo[de]isoquinoline-1,3(2H)-dione (13):** Yellow solid, *E/Z* 1:1.4; Yield 71%; mp: 238–242 °C; <sup>1</sup>H NMR (400 MHz, CDCl<sub>3</sub>): δ = 8.63–8.61 (d, *J* = 7.24 Hz, 1H, ArH), 8.57–8.55 (d, *J* = 7.16 Hz, 1H, ArH), 8.50–8.42 (m, 2H, ArH), 8.13–8.07 (m, 1H, ArH), 7.70–7.59 (m, 2H, ArH), 7.41–7.34 (m, 4H, ArH), 7.31–7.28 (m, 5H, ArH), 7.23–7.22 (m, 5H, ArH), 7.17–7.07 (m, 6H, ArH), 7.05–7.01 (m, 5H, ArH), 6.96–6.94 (m, 4H, ArH), 3.64 (brs, 2H, cyclohexyl-NH), 3.14 (s, 1H, cyclohexyl-CH), 3.11 (s, 1H, cyclohexyl-CH), 2.23 (s, 3H, CH<sub>3</sub>), 2.16 (s, 3H, CH<sub>3</sub>), 1.88–1.85 (m, 3H, cyclohexyl-CH<sub>2</sub>), 1.76–1.72 (m, 2H, cyclohexyl-CH<sub>2</sub>), 1.42–1.33 (m, 7H, cyclohexyl-CH<sub>2</sub>), 1.29–1.28 (m, 2H, cyclohexyl-CH<sub>2</sub>), 1.25–1.21 (m, 6H, cyclohexyl-CH<sub>2</sub>); <sup>13</sup>C NMR (100 MHz, CDCl<sub>3</sub>): δ = 165.0, 164.8, 164.3, 164.2, 148.7, 148.6, 144.1, 143.7, 143.4, 143.3, 143.0, 142.8, 138.8, 138.7, 136.4, 136.3, 134.9, 134.8, 133.6, 131.7, 131.6, 131.5, 131.2, 131.1, 130.9, 130.6, 130.5, 130.4, 130.3, 129.4, 128.5, 128.3, 128.2, 128.1, 127.9, 127.7, 127.6, 127.5, 126.8, 126.7, 126.6, 126.5, 126.2, 126.1, 125.9, 124.7, 124.6, 123.4, 123.3, 120.2 (ArC), 51.8 (cyclohexyl-CH), 32.8 (cyclohexyl-CH<sub>2</sub>), 25.7 (cyclohexyl-CH<sub>2</sub>), 24.9 (cyclohexyl-CH<sub>2</sub>), 23.7 (CH<sub>3</sub>), 23.6 (CH<sub>3</sub>); HRMS (TOF MS): *m/z* calcd C<sub>39</sub>H<sub>34</sub>N<sub>2</sub>O<sub>2</sub> 563.2620, found 563.2623.

**2-(4-(1,2-Diphenylprop-1-en-1-yl)-6-((2-morpholinoethyl)amino)-1H-benzo[de]isoquinoline-1,3(2H)-dione (14):** Yellow solid, *E/Z* 1:1; yield 62%; mp: 249–252 °C; <sup>1</sup>H NMR (500 MHz, CDCl<sub>3</sub>): δ = 8.65–8.64 (d, *J* = 7.20 Hz, 1H, ArH), 8.59–8.57 (d, *J* = 7.25 Hz, 1H, ArH), 8.52–8.50 (d, *J* = 8.3 Hz, 1H, ArH), 8.46–8.44 (d, *J* = 8.35 Hz, 2H, ArH), 8.18–8.12 (m, 2H, ArH), 7.71–7.64 (m, 2H, ArH), 7.41–7.35 (m, 4H, ArH), 7.32–7.28 (m, 5H, ArH), 7.23–7.20 (m, 4H, ArH), 7.17–7.10 (m, 6H, ArH), 7.04–7.00 (m, 5H, ArH), 6.96–6.95 (m, 4H, ArH), 6.37 (brs, 1H, NH), 6.33 (brs, 1H, NH), 3.79 (brs, 8H, morph-OCH<sub>2</sub>), 3.47–3.40 (m, 4H, ethyl-NHCH<sub>2</sub>), 2.86–2.80 (m, 4H, ethyl-CH<sub>2</sub>), 2.59 (brs, 8H, morph-NCH<sub>2</sub>), 2.23 (s, 3H, CH<sub>3</sub>), 2.17 (s, 3H, CH<sub>3</sub>); <sup>13</sup>C NMR (100 MHz, CDCl<sub>3</sub>): δ = 165.0, 164.8, 149.7, 149.6, 144.1, 143.7, 143.3, 142.8, 138.8, 138.7, 136.4, 136.3, 135.0, 134.8, 134.3, 133.5, 131.6, 131.5, 131.2, 131.1, 131.0, 130.9, 130.3, 130.2, 129.4, 128.5, 128.2, 128.1, 127.9, 127.7, 127.5, 126.7, 126.6, 126.2, 125.9, 125.2, 125.1, 125.0, 123.4, 123.3, 120.6, 120.5, 120.1, 110.3 (ArC), 67.1 (morph-OC), 67.0 (morph-OC), 56.0 (aliphatic-NC), 55.9 (aliphatic-NC), 53.2 (ethyl-NC), 53.1 (ethyl-NC), 23.7 (CH<sub>3</sub>), 23.6 (CH<sub>3</sub>); HRMS (TOF MS): *m/z* calcd C<sub>39</sub>H<sub>35</sub>N<sub>3</sub>O<sub>3</sub> 594.2678, found 594.2650.

**6-(2-(Dimethylamino)ethylamino)-2-(4-(1,2-diphenylprop-en-1-yl)phenyl)-1H-benzo[de]isoquinoline-1,3(2H)-dione (15):** Yellow

solid, *E/Z* 1:1.3; Yield 68%; mp: 233–235 °C; <sup>1</sup>H NMR (500 MHz, CDCl<sub>3</sub>): δ = 8.61–8.59 (d, *J* = 7.15 Hz, 1H, ArH), 8.54–8.53 (d, *J* = 7.25 Hz, 1H, ArH), 8.50–8.48 (d, *J* = 8.30 Hz, 1H, ArH), 8.44–8.42 (d, *J* = 8.30 Hz, 1H, ArH), 8.30–8.25 (m, 2H, ArH), 7.63–7.56 (m, 2H, ArH), 7.40–7.35 (m, 4H, ArH), 7.31–7.28 (m, 5H, ArH), 7.23–7.20 (m, 5H, ArH), 7.17–7.09 (m, 5H, ArH), 7.05–7.01 (m, 4H, ArH), 6.96–6.93 (m, 3H, ArH), 3.91–3.88 (m, 4H, ethyl-NCH<sub>2</sub>), 3.83–3.80 (m, 4H, ethyl-NCH<sub>2</sub>), 3.43 (s, 4H, CH<sub>3</sub>), 3.41 (s, 6H, CH<sub>3</sub>), 2.23 (s, 3H, CH<sub>3</sub>), 2.16 (s, 3H, CH<sub>3</sub>); <sup>13</sup>C NMR (100 MHz, CDCl<sub>3</sub>): δ = 165.1, 164.9, 164.5, 164.4, 149.9, 149.8, 144.0, 143.7, 143.4, 143.3, 142.9, 142.8, 138.8, 138.6, 136.4, 134.8, 134.7, 134.4, 133.6, 131.6, 131.5, 131.1, 130.8, 130.3, 130.2, 129.3, 128.5, 128.2, 128.1, 127.9, 127.8, 127.5, 126.7, 126.6, 126.2, 125.9, 125.2, 125.1, 122.8, 120.9, 110.0 (ArC), 59.0 (ethyl-NHCH<sub>2</sub>), 45.0 (ethyl-NCH<sub>2</sub>), 44.8 (ethyl-NCH<sub>2</sub>), 40.1 (NCH<sub>3</sub>) 40.0 (NCH<sub>3</sub>), 23.7 (CH<sub>3</sub>), 23.6 (CH<sub>3</sub>); HRMS (TOF MS): *m/z* calcd C<sub>37</sub>H<sub>33</sub>N<sub>3</sub>O<sub>2</sub> 552.2573, found 552.2545.

**6-(Butylamino)-2-(4-(1,2-diphenylprop-1-en-yl)phenyl)-1H-benzo [de] isoquinoline-1,3(2H)-dione (16):** Yellow solid, *E/Z* 1:1; Yield 60%; mp: 245–248 °C; <sup>1</sup>H NMR (500 MHz, CDCl<sub>3</sub>): δ = 8.64–8.62 (m, *J* = 7.20 Hz, 1H, ArH), 8.59–8.56 (m, 1H, ArH), 8.52–8.49 (m, 1H, ArH), 8.48–8.44 (m, 1H, ArH), 8.14–8.06 (m, 2H, ArH), 7.72–7.59 (m, 2H, ArH), 7.41–7.35 (m, 3H, ArH), 7.31–7.28 (m, 5H, ArH), 7.23–7.23 (m, 5H, ArH), 7.17–7.08 (m, 6H, ArH), 7.06–7.02 (m, 4H, ArH), 6.96–6.92 (m, 3H, ArH), 6.78–6.72 (m, 2H, ArH), 4.16 (brs, 2H, NH), 3.45–3.41 (m, 4H, butyl-NCH<sub>2</sub>), 2.23 (s, 3H, CH<sub>3</sub>), 2.16 (s, 3H, CH<sub>3</sub>), 1.86–1.77 (m, 4H, butyl-CH<sub>2</sub>), 1.73–1.67 (m, 4H, butyl-CH<sub>2</sub>), 0.89–0.86 (m, 4H, butyl-CH<sub>2</sub>); <sup>13</sup>C NMR (100 MHz, CDCl<sub>3</sub>): δ = 165.0, 164.9, 164.5, 164.4, 164.3, 164.2, 150.0, 149.9, 149.8, 144.2, 144.1, 143.8, 143.7, 143.4, 143.3, 142.9, 142.8, 138.9, 138.8, 138.7, 138.6, 136.4, 136.3, 136.2, 135.1, 135.0, 134.9, 134.4, 134.3, 133.6, 133.5, 131.6, 131.1, 130.9, 130.3, 130.2, 129.4, 128.5, 128.3, 128.2, 128.1, 127.9, 127.7, 127.5, 126.7, 126.6, 126.4, 126.3, 125.9, 124.9, 124.8, 124.7, 124.6, 123.4, 123.3, 120.3, 120.2, 110.1, 110.0 (ArC), 43.5 (butyl-NC), 43.4 (butyl-NC), 31.1 (butyl-C), 31.0 (butyl-C), 23.7 (CH<sub>3</sub>), 23.6 (CH<sub>3</sub>), 20.5 (butyl-C), 20.4 (butyl-C), 14.0 (butyl-C), 13.9 (butyl-C); HRMS (TOF MS): *m/z* calcd C<sub>37</sub>H<sub>32</sub>N<sub>2</sub>O<sub>2</sub> 537.2464, found 537.2438.

**2-(4-(1,2-Diphenylprop-1-en-yl)phenyl)-6-((2-hydroxyethyl) amino)-1H-benzo[de]isoquinoline-1,3(2H)-dione (17):** Yellow solid, *E/Z* 1:3; Yield 63%; mp: 232–235 °C; <sup>1</sup>H NMR (500 MHz, CDCl<sub>3</sub>): δ = 8.63–8.43 (m, 3H, ArH), 8.18–8.15 (m, 1H, ArH), 7.70–7.58 (m, 2H, ArH), 7.46–7.35 (m, 3H, ArH), 7.32–7.28 (m, 4H, ArH), 7.23–7.20 (m, 4H, ArH), 7.17–7.10 (m, 3H, ArH), 7.04–7.02 (m, 3H, ArH), 6.96–6.93 (m, 2H, ArH), 6.79–6.71 (m, 1H, ArH), 5.79 (brs, 2H, OH), 4.45 (brs, 1H, NH), 4.05 (brs, 2H, ethyl-OCH<sub>2</sub>), 3.97 (brs, 1H, ethyl-OCH<sub>2</sub>), 3.58 (brs, 3H, ethyl-NCH<sub>2</sub>), 2.23 (s, 3H, CH<sub>3</sub>), 2.16 (s, 3H, CH<sub>3</sub>); <sup>13</sup>C NMR (100 MHz, CDCl<sub>3</sub>): δ = 165.0, 164.8, 164.4, 164.3, 144.9, 144.8, 144.6, 144.5, 144.2, 144.1, 143.8, 143.7, 143.3, 143.0, 142.8, 132.0, 131.6, 131.2, 131.0, 130.2, 130.1, 129.4, 128.2, 128.1, 128.0, 127.9, 127.8, 127.7, 127.3, 126.7, 126.6, 126.4, 126.0, 123.0, 120.5, 114.7, 114.3, 110.4, 110.3, 104.6, 104.5 (ArC), 60.5 (CH<sub>2</sub>OH), 60.4 (CH<sub>2</sub>OH), 45.4 (NCH<sub>2</sub>), 45.3 (NCH<sub>2</sub>), 23.5 (CH<sub>3</sub>), 23.4 (CH<sub>3</sub>); HRMS (TOF MS): *m/z* calcd C<sub>35</sub>H<sub>28</sub>N<sub>2</sub>O<sub>3</sub> 525.2100, found 525.2173.

**6-(Allylamino)-2-(4-(1,2-diphenylprop-1-en-1 yl)phenyl)-1H-benzo [d e]iso quinoline-1,3 (2H)-dione (18):** Yellow solid, *E/Z* 1:1.8; Yield 72%; mp: 230–234 °C; <sup>1</sup>H NMR (500 MHz, CDCl<sub>3</sub>): δ = 8.65–8.57 (m, 2H, ArH), 8.52–8.44 (m, 2H, ArH), 8.18–8.11 (m, 2H, ArH), 7.70–7.63 (m, 2H, ArH), 7.41–7.35 (m, 4H, ArH), 7.31–7.28 (m, 5H, ArH), 7.23 (m, 3H, ArH), 7.17–7.16 (m, 3H, ArH), 7.03–7.02 (m, 3H, ArH), 6.96–6.93 (m, 2H, ArH), 6.79–6.74 (m, 2H, ArH), 6.04 (brs, 2H, NH), 5.45–5.37 (m, 2H, allyl-CH), 5.35–5.27 (m, 2H, allyl-CH<sub>2</sub>), 5.19–5.17 (d, *J* = 10.15 Hz, 1H, allyl-CH<sub>2</sub>), 4.80–4.73 (m, 1H, allyl-CH<sub>2</sub>), 4.11–4.02 (m, 4H, allyl-NCH<sub>2</sub>), 2.23 (s, 3H, CH<sub>3</sub>), 2.16 (s, 3H, CH<sub>3</sub>); <sup>13</sup>C NMR (100 MHz, CDCl<sub>3</sub>): δ = 165.0, 164.8, 164.5, 164.4, 164.2, 163.9, 144.1, 143.7, 143.4, 143.3, 142.9, 142.8, 138.8, 138.6, 136.4, 134.8, 134.7, 134.6, 134.2, 133.5, 133.0, 131.6, 131.5, 131.3, 131.1, 130.9, 130.2,

129.9, 129.4, 128.5, 128.2, 128.1, 127.9, 127.7, 127.5, 126.7, 126.6, 126.4, 126.3, 126.2, 125.9, 125.0, 124.9, 124.8, 123.4, 123.3, 123.1, 120.5, 120.4, 120.3, 118.1, 118.0, 117.1, 110.7, 110.6 (ArC), 46.2 (allyl-NC), 46.1 (allyl-NC), 23.7 (CH<sub>3</sub>), 23.6 (CH<sub>3</sub>); HRMS (TOF MS): *m/z* calcd C<sub>36</sub>H<sub>28</sub>N<sub>2</sub>O<sub>2</sub> 521.2151, found 521.2177.

**6-(Benzylamino)-2-(4-(1,2-diphenylprop-1-en-yl)phenyl)-1H-benzo [de]isoquinoline-1,3(2H)-dione (19):** Yellow solid, *E/Z* 1:1.2; Yield 65%; mp: 244–248 °C; <sup>1</sup>H NMR (400 MHz, CDCl<sub>3</sub>): δ = 8.65–8.62 (d, *J* = 7.30 Hz, 1H, ArH), 8.59–8.57 (d, *J* = 7.25 Hz, 1H, ArH), 8.51–8.49 (d, *J* = 8.35 Hz, 1H, ArH), 8.45–8.41 (d, *J* = 8.35 Hz, 1H, ArH), 8.18–8.12 (m, 2H, ArH), 7.69–7.62 (m, 2H, ArH), 7.43–7.35 (m, 13H, ArH), 7.31–7.28 (m, 5H, ArH), 7.23–7.20 (m, 4H, ArH), 7.17–7.11 (m, 5H, ArH), 7.03–7.00 (m, 4H, ArH), 6.96–6.92 (m, 3H, ArH), 6.83–6.77 (m, 2H, ArH), 5.62 (brs, 1H, NH), 5.55 (brs, 1H, NH), 4.65–4.61 (m, 4H, benzyl-NCH<sub>2</sub>), 2.23 (s, 3H, CH<sub>3</sub>), 2.16 (s, 3H, CH<sub>3</sub>); <sup>13</sup>C NMR (100 MHz, CDCl<sub>3</sub>): δ = 165.0, 164.8, 164.4, 164.2, 144.0, 143.7, 143.4, 143.3, 142.9, 142.8, 138.8, 138.6, 137.1, 136.4, 134.9, 134.7, 134.2, 133.4, 131.6, 131.5, 131.1, 130.9, 130.2, 129.4, 129.2, 129.1, 128.2, 128.1, 127.9, 127.6, 127.5, 126.7, 126.6, 126.5, 126.3, 125.9, 125.1, 125.0, 123.3, 120.5, 120.4, 110.7 (ArC), 48.0 (benzyl-CH<sub>2</sub>), 47.9 (benzyl-CH<sub>2</sub>), 23.7 (CH<sub>3</sub>), 23.6 (CH<sub>3</sub>); HRMS (TOF MS): *m/z* calcd C<sub>40</sub>H<sub>30</sub>N<sub>2</sub>O<sub>2</sub> 571.2307, found 571.2381.

**2-(4-(1,2-Diphenylprop-1-en-1-yl)phenyl)-6-((4-fluorophenyl) amino)-1H-benzo[de]isoquinoline-1,3(2H)-dione (20):** Yellow solid, *E/Z* 1:4.8; Yield 61%; mp: 232–234 °C; <sup>1</sup>H NMR (400 MHz, CDCl<sub>3</sub>): δ = 8.70–8.58 (m, 2H, ArH), 8.45–8.38 (m, 1H, ArH), 8.09–8.03 (m, 1H, ArH), 7.90–7.82 (m, 1H, ArH), 7.40–7.27 (m, 7H, ArH), 7.24–7.21 (m, 3H, ArH), 7.16–7.10 (m, 5H, ArH), 7.05–6.93 (m, 6H, ArH), 6.66–6.63 (m, 2H, ArH), 6.35–6.33 (d, *J* = 8.40 Hz, 1H, ArH), 3.13 (brs, 1H, NH), 3.10 (brs, 1H, NH), 2.21 (s, 1H, CH<sub>3</sub>), 2.16 (s, 1H, CH<sub>3</sub>); <sup>13</sup>C NMR (100 MHz, CDCl<sub>3</sub>): δ = 163.9, 163.8, 163.7, 155.8, 144.9, 144.6, 144.5, 144.2, 144.1, 143.7, 143.6, 143.4, 143.3, 139.3, 139.1, 138.5, 136.7, 136.6, 134.7, 134.0, 132.6, 132.4, 132.0, 131.8, 131.8, 131.7, 131.6, 131.3, 131.2, 131.0, 130.2, 130.1, 129.5, 129.4, 129.3, 128.3, 128.2, 128.1, 128.0, 127.9, 127.8, 127.7, 127.5, 127.3, 126.8, 126.7, 126.6, 126.4, 126.0, 125.9, 125.7, 114.7, 114.3 (ArC), 23.7 (CH<sub>3</sub>), 23.6 (CH<sub>3</sub>); HRMS (TOF MS): *m/z* calcd C<sub>39</sub>H<sub>27</sub>FN<sub>2</sub>O<sub>2</sub> 575.2057, found 575.2051.

**2-(4-(1,2-Diphenylprop-1-en-1-yl)phenyl)-6-(pyrimidin-2-ylami- no)-1H-benzo[de]isoquinoline-1,3(2H)-dione (21):** Yellow solid, *E/Z* 1:1.5; Yield 67%; mp: 232–235 °C; <sup>1</sup>H NMR (500 MHz, CDCl<sub>3</sub>): δ = 8.71–8.42 (m, 5H, ArH), 7.80–7.76 (m, 3H, ArH), 7.45–7.29 (m, 9H, ArH), 7.21–7.12 (m, 6H, ArH), 7.10–7.05 (m, 5H, ArH), 7.03–7.01 (m, 5H, ArH), 6.95–6.92 (m, 3H, ArH), 2.21 (s, 2H, CH<sub>3</sub>), 2.15 (s, 3H, CH<sub>3</sub>); <sup>13</sup>C NMR (100 MHz, CDCl<sub>3</sub> + [D<sub>6</sub>]DMSO): δ = 164.9, 164.8, 164.3, 164.2, 160.8, 143.6, 143.3, 143.2, 142.8, 142.7, 138.5, 136.3, 134.2, 134.1, 133.4, 131.8, 131.5, 131.1, 130.7, 130.1, 129.7, 129.6, 129.3, 128.4, 128.2, 128.0, 127.8, 127.7, 127.4, 126.6, 126.5, 126.2, 125.9, 125.3, 125.2, 123.1, 123.0, 122.3, 113.4, 110.2, 110.1 (ArC), 23.6 (CH<sub>3</sub>), 23.5 (CH<sub>3</sub>); HRMS (TOF MS): *m/z* calcd C<sub>37</sub>H<sub>26</sub>N<sub>4</sub>O<sub>2</sub> 559.2056, found 559.2050.

## HPLC chromatography

To analyze the ratio of *E* and *Z* isomers of the TPE-naphthalimide conjugate, reversed-phase (RP) HPLC has been performed using Ultimate 3000 HPLC (ThermoFisher Scientific) system, equipped with C-18 column (250 × 4.6 mm, 5 mm) and UV/Vis detector. The wavelength used was 400 nm and the mobile phase was comprised of 0.01 M tetrabutylammoniumhydrogensulfate/acetonitrile (30:70 *v/v*) with flow rate 1.0 mL/min. The stock solution of *E/Z* of TPE-naphthalimide conjugate derivative, that is, **7** (1 mM) was prepared in acetonitrile and protected from direct light. The stock solution was then diluted to produce a solution of compound in acetonitrile (2.3 × 10<sup>-4</sup> M). First, the prepared sample was filtrated using

0.22  $\mu\text{m}$  cellulose filtrate. Then, 20  $\mu\text{L}$  of the filtered sample was injected into the column with an injection loop.

### In vitro antitumor activity

National Cancer Institute, USA selected the TPE-naph conjugates on account of computer modeling studies. Further, these newly synthesized derivatives were tested for their anticancer activity against 60 human cancer cell lines at 10  $\mu\text{M}$  concentration by a standard procedure.

### Topoisomerase-II inhibitory assay

Relaxation of supercoiled plasmid DNA by TOPO-II $\alpha$  was assayed in 20  $\mu\text{L}$  of buffer (0.5 M Tris-HCl (pH 8.0), 1.5 M NaCl, 100 mM  $\text{MgCl}_2$ , 20 mM ATP, 5 mM dithiothreitol, 300  $\mu\text{g}/\text{mL}$  BSA) containing drug solution, 4 U of DNA topoisomerase-II $\alpha$  and 500 ng of supercoiled pHOT1 plasmid DNA and incubated at 37  $^\circ\text{C}$  for 30 min. Reactions were terminated by the addition of 2  $\mu\text{L}$  of a solution containing 10% sodium dodecyl sulfate (SDS) and 0.5 mg/mL of proteinase K and incubated at 37  $^\circ\text{C}$  for 30 min. Then, 1  $\mu\text{L}$  of loading buffer (50% glycerol and 0.25% bromophenol blue) was added. The samples were electrophoresed in 1% agarose gel with TAE buffer (100 mL of 10 stock solution-4.8 g of tris base, 1.14 mL acetic acid, and 0.37 g EDTA, pH 8.1) for 4 h, then the DNA was stained with ethidium bromide and photographed under UV illuminator.

### Time-resolved fluorescence measurement

Time-resolved fluorescence decay measurements were carried out by modulator time fluorescence system on deltaflex spectrometer. A pulsed diode ( $\lambda_{\text{max}} = 280 \text{ nm}$ ) was used as the excitation source, and emission was monitored at respective emission wavelengths. The data was analyzed by using Horiba EZ software attached with the system.

### Molecular modeling

Molecular docking studies were employed to authenticate the interaction between ligand and TOPO-II-DNA complex using software AutoDock 4.0. The three-dimensional X-ray structure of topoisomerase-II-DNA-etoposide ternary complex was retrieved from the protein data bank (PDB ID: 5GWK). Etoposide was excluded from ternary complex to perform the docking. To setup ligand TOPO-II interaction, AutoDock tools 1.5.6rc3 was accomplished to remove the water molecules, add the polar hydrogen atoms. As well gasteiger charges were computed and hydrogen atoms which are nonpolar were merged to carbon atoms. The 3D structures of the molecules were kept in PDB format with aid of Gaussian 09 W program. Using ADT package (version 1.5.6rc3), the PDB file was further modified for partial charges. The charges of the nonpolar hydrogen atoms have been assigned to the atom to which hydrogen is attached and file was saved as Pdbqt file. The docking put files were generate by using the AutoDockTools program. A cubic grid dimension 60  $\text{\AA} \times 60 \text{\AA} \times 60 \text{\AA}$  with the grid points along the x, y and z axes and a grid spacing of 0.375  $\text{\AA}$  was used. The optimized cluster was classified with minimum energy level in the best suitable conformation of TOPO-II-DNA-ligand modeled structure. The molecular structures were analyzed using Discovery studio.

### Acknowledgments

KP thanks the CSIR, New Delhi [(02(0310)/17/EMR-II) and SERB, New Delhi (CRG/2018/002159) for financial support. The authors express their gratitude to NCI, NIH for antiproliferative activity.

### Conflict of Interest

The authors declare no conflict of interest.

**Keywords:** anticancer activity · human serum albumin · naphthalimide · topoisomerase · triphenylethylene

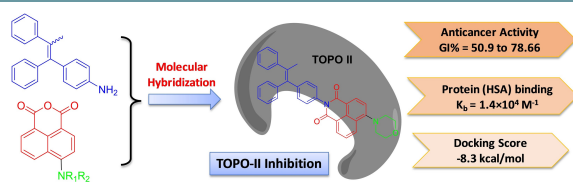
- [1] L. A. Torre, R. L. Siegel, E. M. Ward, A. Jemal, *Cancer Epidemiol. Biomarkers Prev.* **2016**, *25*, 16–27.
- [2] J. Ferlay, M. Colombet, I. Soerjomataram, C. Mathers, D. M. Parkin, M. Pineros, A. Znaor, F. Bray, *Int. J. Cancer.* **2019**, *144*, 1941–1953.
- [3] K. Dhingra, *Ann. Oncol.* **2015**, *26*, 2347–2350.
- [4] M. Nikolaou, A. Pavlopoulou, A. G. Georgakilas, E. Kyrodimos, *Clin. Exp. Metastasis* **2018**, *35*, 309–318.
- [5] a) R. J. Sunil, P. Sarbani, A. Jayashree, *Med. Chem.* **2019**, *9*, 93–95; b) C. V. Junior, A. Danuello, V. D. S. Bolzani, E. J. Barreiro, C. A. M. Fraga, *Curr. Med. Chem.* **2007**, *14*, 1829–1852.
- [6] Shagufta, I. Ahmad, *Eur. J. Med. Chem.* **2018**, *143*, 515–531.
- [7] R. Tandon, V. Luxami, H. Kaur, N. Tandon, K. Paul, *Chem. Rec.* **2017**, *17*, 956–993.
- [8] V. C. Jordan, B. W. O'Malley, *J. Clin. Oncol.* **2007**, *25*, 5815–5824.
- [9] V. C. Jordan, *Nat. Rev. Drug Discovery* **2003**, *2*, 205–213.
- [10] H. K. Patel, T. Bihan, *Pharmacol. Ther.* **2018**, *186*, 1–24.
- [11] S. Rani, K. Paul, *Eur. J. Med. Chem.* **2020**, *208*, 112775–112786.
- [12] J. Iqbal, O. M. Ginsburg, T. D. Wijeratne, A. Howell, G. Evans, I. Sestak, S. A. Narod, *Cancer Treat. Rev.* **2012**, *38*, 318–328.
- [13] G. Tan, Y. Yao, Y. Gu, S. Li, M. Lv, K. Wang, H. Chen, X. Li, *Bioorg. Med. Chem. Lett.* **2014**, *24*, 2825–2830.
- [14] E. Catanzaro, F. Seghetti, C. Calcabrini, A. Rampa, S. Gobbi, P. Sestili, E. Turrini, F. Maffei, P. Hrelia, A. Bisi, F. Belluti, C. Bioorg. Chem. **2019**, *86*, 538–549.
- [15] H. H. Gong, D. Addla, J. S. Lv, C. H. Zhou, *Curr. Top. Med. Chem.* **2016**, *16*, 3303–3364.
- [16] Shalini, Pankaj, S. T. Saha, M. Kaur, E. Oluwakemi, P. Awolade, P. Singh, V. Kumar, *RSC Adv.* **2020**, *10*, 15836–15845.
- [17] I. Singh, V. Luxami, K. Paul, *Bioorg. Chem.* **2020**, *96*, 103631.
- [18] T. Brider, B. Redko, F. Grynszpan, G. Gellerman, *Tetrahedron Lett.* **2014**, *55*, 6675–6679.
- [19] M. F. Brana, A. Ramos, *Curr. Med. Chem. Anti-Cancer Agents* **2001**, *1*, 237–255.
- [20] M. J. Ratain, R. Mick, F. Berezin, L. Janisch, R. L. Schilsky, N. J. Vogelzang, L. B. Lane, *Cancer Res.* **1993**, *53*, 2304–2308.
- [21] N. S. Rao, N. Nagesh, V. L. Nayak, S. Sunkari, R. Tokala, G. Kiranmai, P. Regur, N. Shankaraiah, A. Kamal, *MedChemComm* **2019**, *10*, 72–79.
- [22] Y. T. Lu, T. L. Chen, K. S. Chang, C. M. Chang, T. Y. Wei, J. W. Liu, C. A. Hsiao, T. L. Shih, *Bioorg. Med. Chem.* **2017**, *25*, 789–794.
- [23] R. P. Tanpure, A. R. Harkrider, T. E. Strecker, E. Hamel, M. L. Trawick, K. G. Pinney, *Bioorg. Med. Chem.* **2009**, *17*, 6993–7001.
- [24] M. S. R. Marty, M. R. Katiki, J. B. Nanubolu, S. Garimella, S. Polepalli, N. Jain, A. K. Buddana, R. S. Prakasham, *Mol. Diversity* **2016**, *20*, 687–703.
- [25] G. R. Bedford, D. N. Richardson, *Nature* **1966**, *212*, 733–734.
- [26] J. Shani, A. Gazit, T. Livshitz, S. Biran, *J. Med. Chem.* **1985**, *28*, 1504–1511.
- [27] M. R. Boyd, K. D. Paull, *Drug Dev. Res.* **1995**, *34*, 91–109.
- [28] W. Hu, X. S. Huang, J. F. Wu, L. Yang, Y. T. Zheng, Y. M. Shen, Z. Li, X. Li, *J. Med. Chem.* **2018**, *61*, 8947–8980.
- [29] S. K. Maddili, R. Katla, V. K. Kannekanti, N. K. Bejjanki, B. Tuniki, C. H. Zhou, H. Gandham, *Eur. J. Med. Chem.* **2018**, *150*, 228–247.
- [30] V. D. Suryawanshi, P. V. Anbhule, A. H. Gore, S. R. Patil, G. B. Kolekar, *Ind. Eng. Chem. Res.* **2012**, *51*, 95–102.
- [31] H. A. Benesi, J. H. Hildebrand, *J. Am. Chem. Soc.* **1949**, *71*, 2703–2707.
- [32] J. R. Lakowicz, *Principles of Fluorescence Spectroscopy*, 3rd ed. Springer, New York, **2006**.

- [33] J. R. Lakowicz, G. Webber, *Biochemistry* **1973**, *12*, 4161–4170.
- [34] M. R. Eftink, C. A. Ghiron, *Anal. Biochem.* **1981**, *114*, 199–227.
- [35] G. Scatchard, *N. Y. Ann. Acad. Sci.* **1949**, *51*, 660–672.
- [36] I. Singh, V. Luxami, K. Paul, *Org. Biomol. Chem.* **2019**, *17*, 5349–5366.
- [37] L. Zhao, J. Liu, R. Guo, Q. Sun, H. Yang, H. Li, *RSC Adv.* **2017**, *7*, 27796–27806.
- [38] G. M. Morris, R. Huey, W. Lindstorm, M. F. Sanner, R. K. Belew, D. S. Goodsell, A. J. Olson, *J. Comput. Chem.* **2009**, *30*, 2785–2791.
- [39] S. D. Ross, M. Finkelstein, R. C. Petersen, *J. Am. Chem. Soc.* **1958**, *80*, 4327–4330.
- [40] P. H. Grayshan, A. M. Kadhim, A. T. Peters, *J. Heterocycl. Chem.* **1974**, *11*, 33–38.

---

Manuscript received: January 15, 2021  
Revised manuscript received: February 18, 2021  
Accepted manuscript online: March 16, 2021  
Version of record online: ■■■, ■■■■

## FULL PAPERS



**Anticancer amines:** Triphenylethylene-naphthalimide hybrids were synthesized and screened for activity against 60 human cancer cell lines. The compound with a morpholine group exhibited broad-spectrum anticancer

activity at  $-11.3 \mu\text{M}$  and was found to be more cytotoxic than amonafide against four cancer cell lines. It displayed inhibitory activity against topoisomerase-II $\alpha$  and remarkable binding affinity towards HSA.

*S. Rani, Dr. V. Luxami, Dr. K. Paul\**

1 – 12

**Synthesis of Triphenylethylene-Naphthalimide Conjugates as topoisomerase-II $\alpha$  inhibitor and HSA binder**

